Composition, Demographic History, and Population Structures of *Trichiurus*

Kui-Ching Hsu [1†], Mu-Rong Yi [1,2†], Sui Gu [1], Xiong-Bo He [1,2], Zhi-Sen Luo [1], Bin Kang [3], Hung-Du Lin [4*] and Yun-Rong Yan [1,2,5,6*]

[1] College of Fisheries, Guangdong Ocean University, Zhanjiang, China, [2] Marine Resources Big Data Center of South China Sea, Southern Marine Science and Engineering Guangdong Laboratory, Zhanjiang, China, [3] Fisheries College, Ocean University of China, Qingdao, China, [4] Department of Biology, The Affiliated School of National Tainan First Senior High School, Tainan, Taiwan, [5] Guangdong Provincial Engineering and Technology Research Center of Far Sea Fisheries Management and Fishing of South China Sea, Guangdong Ocean University, Zhanjiang, China, [6] Center of Marine Fisheries Information Technology, Shenzhen Institute of Guangdong Ocean University, Shenzhen, China

Sequences of the complete mitochondrial cytochrome oxidase subunit I gene were used to identify *Trichiurus* species and examine their population genetic structure and demographic history along the coast of China. Three *Trichiurus* species were found. *Trichiurus japonicus* lives in colder waters along the continental shelves in the China Seas, while *Trichiurus nanhaiensis* lives warmer waters along continental slopes in the South China Sea, and *Trichiurus brevis* lives in shallow and warmer waters in the South China Sea. The migrations of these species were mainly associated with feeding and spawning preferences. Two major wintering and spawning grounds in the East China Sea and South China Sea were found. All species showed a lack of population genetic structure resulting from their oceanodromous life cycle (the degree of population substructure index N_{ST} = 0.000–0.149), but the results of approximate Bayesian computational approaches suggested population declines or stabilization and differentiation. The results of the T_{MRCA} (time to the most recent common ancestor) showed that during glaciations, the Yellow Sea and the East China Sea were completely exposed, and the South China Sea acted as a refugium. Thus, the populations of these three species experienced differentiation during glaciations. This study also examined the limitations of Bayesian skyline plot analysis.

Keywords: habitat characterization, oceanographic conditions, Pleistocene, species composition, wintering ground

INTRODUCTION

Marine fisheries, namely, capture fisheries and aquacultural operations, are sources of nutrients for improving human health and play a critical role in sustaining marine ecosystem function (FAO, 2016). China has the largest fishing production in the world. After the mid-1990s, the estimated total annual production of its fisheries accounted for 30% of global fisheries production, and currently, its aquaculture accounts for more than 60% of global aquaculture production (FAO, 2012;

FAO, 2016). Hairtail fish, belonging to the genus *Trichiurus* (Dai-yu in Chinese), are the largest component of Chinese marine fisheries, but production of this species dramatically declined from 118.68 MT (million ton) in 2010 to 90.85 MT in 2019, with the economic value decreasing from 41.80 billion yuan to 36.93 billion yuan in 2019 (Kang et al., 2018; http://baogao.chinabaogao.com/shuichangqilei/425619425619.html). Thus, it is important to understand the population genetic diversity, structure, and demography of the genus *Trichiurus* to implement resource management policies.

Because hairtail fish are an essential commercial fish in the China Seas, many studies on the systematics, growth, genetic diversity, and demographic history of *Trichiurus* species in the China Seas have been conducted (e.g., Tzeng et al., 2007; Hsu et al., 2009; Shih et al., 2010; He et al., 2014), but some questions about *Trichiurus* species in the China Seas are still unresolved. First, how many species of the genus *Trichiurus* inhabit the China Seas? *Trichiurus* species have similar body appearances and silvery coloration, as well as unresolved taxonomy. There are 31 nominal species in the genus *Trichiurus*, but only nine are valid species (Froese and Pauly, 2021). Many studies have suggested that *Clupea haumela* Fabricius, 1775 is a synonym of *T. lepturus* (e.g., Nakamura and Parin, 1993; Golani and Fricke, 2018; Nakamura and Parin, 2001; Froese and Pauly, 2021). However, a recently published study (Zheng et al., 2019) mentioned this species as a valid *Trichiurus* species without taxonomic evidence and presented its complete mitochondrial genome. Additionally, many studies (e.g., Tucker, 1956; Nakamura and Parin, 1993; Nelson, 1994; Froese and Pauly, 2021) have suggested that *T. japonicus* Temminck and Schlegel, 1844 is synonymous with *T. lepturus*, but other studies (e.g., Lee et al., 1977; Nakabo, 2000; Chakraborty et al., 2006; Tzeng et al., 2007; Hsu et al., 2009; Eschmeyer, 2014; He et al., 2014) have suggested that *T. japonicus* is a valid species. There are thus several outstanding questions regarding the systematics and distributional patterns of *Trichiurus* species. Clear species identification for fishing has been the subject of a major FAO program since the 1960s. Thus, this study surveyed *Trichiurus* species in the China Seas by using morphology and DNA barcoding.

Second, one of the major questions addressed in this study is the population genetic structure and diversity of each *Trichiurus* species along the coastline of China. In contrast to results reported in other allopatric species, many previous studies have proposed genetic differentiation among the Yellow Sea (YS), East China Sea (ECS), and South China Sea (SCS) (Liu et al., 2007; Xu et al., 2009; Zhong et al., 2009). Previous phylogeographic studies have proposed that the population differentiation and speciation in the China Seas were shaped by landform changes during Pliocene and Pleistocene glacial cycles (Kizaki and Oshiro, 1980; Ota, 1994; Wang, 1999; Voris, 2000; Yang et al., 2017; Qu et al., 2018), although some studies found no significant genetic differentiation among the seas (He et al., 2015; Wang X. et al., 2017). Moreover, Jaureguizar et al. (2004) proposed that the major aims of fish migrations are related to seasonal (e.g., *Trichiurus lepturus* and *Discopyge tschudii*) and

reproductive needs (e.g., *Micropogonias furnieri*, *Mustelus schmitti*, and *Cynoscion guatucupa*). Previous studies have suggested that temperature and salinity have the strongest influence on the seasonal structure of species composition (Jaureguizar et al., 2004; Liu et al., 2020; Hou et al., 2021). Thus, our study will investigate the migration patterns of each *Trichiurus* species along the coastline of China and whether these migrations are shaped by environmental factors, including ocean currents. Additionally, He et al. (2014) suggested that cyclic climate changes have shaped the demographic history of two *Trichiurus* species in the China Seas and found that for *T. japonicus* as a whole, a Bayesian skyline plot (BSP) revealed two episodes of population growth, and for *T. nanahaiensis* in the northern SCS, a BSP revealed a steady population decline. However, Kang et al. (2018) proposed that the production of the *Trichiurus* hairtail fish has dramatically declined. Thus, our study examines whether demography has changed and whether some populations are exposed to more pressure based on genetic evidence.

To address the above problems, the mitochondrial DNA (mtDNA) cytochrome c oxidase subunit I (*COI*) gene was used to identify species and investigate the genetic diversity and structure of *Trichiurus* species in the China Seas. Sequences of mtDNA are often analyzed in studies of animal phylogeography (Yang et al., 2016; Chiu et al., 2017; Han et al., 2019). Among all the mtDNA genes, the *COI* gene is the most widely accepted marker for evaluating the levels of genetic diversity and differentiation (Chiu et al., 2017; Wang X. et al., 2017; Liao et al., 2021). Additionally, Hebert et al. (2004) proposed "DNA barcoding" as a way to identify species. The *COI* gene has proven highly effective in identifying birds, butterflies, fishes, and many other animal groups (Hebert et al., 2004). The major questions addressed in our study are as follows: (1) How many *Trichiurus* species are there along the coast of China? (2) What is the current population structure and demography of *Trichiurus* species in the China Seas? The study informed conservation management policies for *Trichiurus* species in the China Seas.

MATERIALS AND METHODS

Sampling and Data Collection

A total of 1,224 specimens of the genus *Trichiurus* were collected from 17 fishing ports in the China Seas in the fall (September and October) of 2018 with longline, gill, and trawl nets by fishermen (**Figure 1A**; **Table 1**). The localities were classified into three seas. Six sampling localities were established off the coast of the YS: (1) Dondog, DD; (2) Dalian, DL; (3) Weihai, WH; (4) Qingdao, QD; (5) Lianyungang, LY; and (6) Nantong, NT. Four sampling localities were established off the coast of the ECS: (7) Zhoushan, ZS; (8) Wenzhou, WZ; (9) Ningde, ND; and (10) Quanzhou, QZ. Seven sampling localities were established off the coast of the SCS: (11) Shantou, ST; (12) Shenzhen, SZ; (13) Yangjiang, YJ; (14) Zhanjiang, ZJ; (15) Beihai, BH; (16) Wenchang, WC; and (17) Sanya, SY (**Table 1**; **Figure 1A**). The *COI* gene was amplified by polymerase chain reaction (PCR)
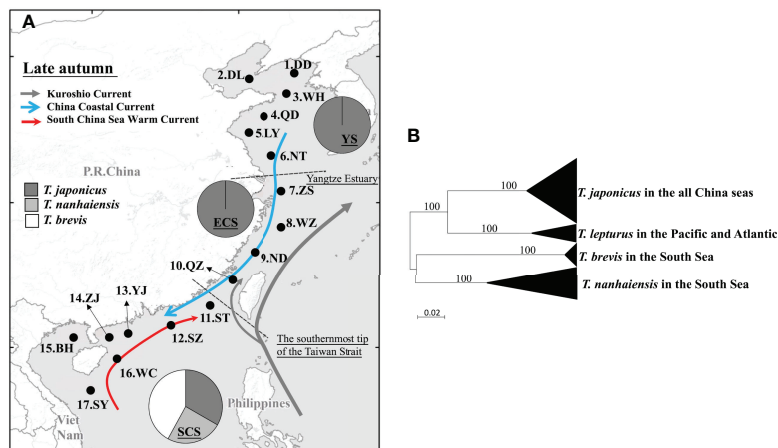
FIGURE 1 | (A) The 17 sampling localities of the genus *Trichiurus* along the coastal areas of the China Seas are indicated by •. See **Table 1** for the site names. The dashed lines represent the boundaries between the Yellow Sea (YS) and the East China Sea (ECS) (Yangtze Estuary), and between the ECS and the South China Sea (SCS). The pie charts represent the species composition of hairtail (*T. japonicus* in dark gray, *T. nanhaiensis* in light gray, and *T. brevis* in white) in three seas. **(B)** The neighbor-joining (NJ) tree of these four *Trichiurus* species is based on the *COI* gene. The numbers at the nodes are bootstrap values. The sampling size (n) is indicated in parentheses.

using the primers Fish-F2 (5'-ACCTCTGTGTGTGGGGCTAC-3') and Fish-R2 (5'-GTGATGCATTGGCTTGAAA-3') (Gu et al., 2021). Each 50 μl PCR mixture contained 5 ng of template DNA, 5 μl of 10× reaction buffer, 4 μl of dNTP mix (10 mM), 5 pmol of each primer and 2 U of Taq polymerase (TaKaRa Biomedical Technology, Beijing). PCR was carried out on an MJ Thermal Cycler with one cycle of denaturation at 94°C for 3 min and 40 cycles of denaturation at 94°C for 30 s, annealing at 51°C for 30 s, and extension at 72°C for 1 min 30 s, followed by a 72°C extension for 10 min and storage at 4°C. The purified PCR products were sequenced using an ABI 377 automated sequencer (Applied Biosystems, Foster City, CA, USA). The chromatograms were checked with Chromas software (Technelysium), and the sequences were manually edited using BioEdit 6.0.7 (Hall, 1999).

Genetic Variability and Structure

The nucleotide sequences were aligned with Clustal X 1.81 (Thompson et al., 1997). The selection of the best-fitting nucleotide substitution models was performed using the Bayesian information criterion (BIC) in jModelTest 2.0 (Darriba et al., 2012). The most appropriate nucleotide substitution model was GTR + I + G. Phylogenetic analysis was used to identify the species in MEGA-X (Kumar et al., 2018). The intrapopulation genetic diversity levels were estimated using haplotype diversity (h) (Nei and Tajima, 1983) and nucleotide diversity (θ_π) indices (Jukes and Cantor, 1969) in DnaSP v5 (Librado and Rozas, 2009). The existence of a phylogeographic structure was examined following the method of Pons and Petit (1996) by calculating the two genetic differentiation indices (G_{ST} and N_{ST}) in DnaSP. G_{ST}, or genetic differentiation among populations, depends only on the frequencies of the haplotypes. N_{ST}, the degree of substructure, is influenced by both haplotype frequencies and the distances between haplotypes.

Demographic History

The demographic histories of hairtail fish were reconstructed using four different approaches. First, we performed Tajima's D and Fu's F_S neutrality tests (Tajima, 1989; Fu, 1997) in DnaSP. Under a population expansion model, significant negative values for Tajima's D and Fu's F_S neutrality tests were expected. Statistical significance was tested using 10,000 permutations. Second, the mismatch distribution (Rogers and Harpending, 1992) was estimated under the assumption of sudden expansion as implemented in Arlequin. The sum of squared deviations (SSD) between observed and expected mismatched distributions, the raggedness index (Rg), and the Ramos-Onsins and Rozas (R2) statistic were used as test statistics with 1,000 bootstrap replicates. In the third approach, we reconstructed historical demography using the coalescent-based Bayesian skyline plot (BSP) approach implemented in BEAST (Drummond et al., 2013). A stick clock model with a Bayesian skyline tree was used. We ran 10^6 generations. The time to the most recent common ancestor (T_{MRCA}) was also calculated using BEAST. A mutation rate of 0.55% per million years (myr) has been estimated for the mtDNA *COI* gene in electric fish (Picq et al., 2014). This rate falls within the range of values previously reported for other freshwater fishes (Webb et al., 2004). The burn-in and plots for each analysis were visualized using Tracer v1.6 (Rambaut et al., 2013) to determine whether the convergence and suitable effective sample sizes were achieved for all parameters. This software was also used to generate skyline plots.

Finally, we performed an approximate Bayesian computation (ABC) with DIYABC v.2.0 software (Cornuet et al., 2014) to detect population size changes and then infer demographic parameters. To examine past transitions in effective population size, our study tested six population demographic scenarios. The scenarios were as follows:

TABLE 1 | Genetic diversity in the species of the genus *Trichiurus* along China Seas.

Locality (Abbr.)	N	H	Hs	Hw	Hd	θ_π	S
T. japonicus	902	521			0.99	0.63	
Yellow Sea (YS)	449	291			0.99	0.62	
1.Dandong (DD)	68	57	35	7	0.99	0.53	0.48
2.Dalian (DL)	91	75	30	9	0.99	0.80	0.82
3.Weihai (WH)	82	62	29	11	0.99	0.55	0.55
4.Qingdao (QD)	95	82	21	8	1.00	0.68	0.51
5.Lianyungang (LY)	33	31	18	2	1.00	0.57	0.46
6.Nantong (NT)	80	64	32	10	0.99	0.49	0.28
East China Sea (ECS)	292	291			1.00	0.63	
7.Zhoushan (ZS)	90	81	36	7	1.00	0.57	0.68
8.Wenzhou (WZ)	69	61	25	6	1.00	0.82	0.32
9.Ningde (ND)	60	53	28	5	1.00	0.55	0.28
10.Quanzhou (QZ)	73	67	27	3	1.00	0.58	0.17
South China Sea (SCS)	161	117			0.99	0.65	
11.Shantou (ST)	4	4	1	0	1.00	0.88	0.70
13.Yangjiang (YJ)	38	35	17	2	0.99	0.75	0.62
14.Zhanjiang (ZJ)	18	18	8	0	1.00	0.56	0.32
15.Beihai (BH)	65	54	23	7	0.99	0.67	0.42
16.Wenchang (WC)	9	3	5	1	0.97	0.42	0.40
17.Sanya (SY)	27	24	17	3	0.99	0.56	0.72
T. nanhaiensis	119	66			0.96	0.29	
11.Shantou (ST)	63	34	5	9	0.93	0.28	
12.Shenzhen (SZ)	52	35	5	5	0.96	0.28	
14.Zhanjiang (ZJ)	4	4	3	0	1.00	0.16	
T. brevis	203	127			0.94	0.27	
11.Shantou (ST)	12	9	3	1	0.91	0.18	
12.Shenzhen (SZ)	53	43	4	2	0.97	0.36	
13.Yangjiang (YJ)	12	11	3	1	0.99	0.22	
15.Beihai (BH)	6	3	1	1	0.60	0.22	
16.Wenchang (WC)	80	54	7	6	0.93	0.23	
17.Sanya (SY)	40	23	8	0	0.86	0.12	
Total	1,224						

N, number of specimens; H, number of haplotypes; Hs, number of haplotypes shared among populations; Hw, number of haplotypes shared within population; Hd, haplotype diversity; θ_π (10^{-2}), nucleotide diversity. The ratio of the empty stomach (S) was also estimated.

In scenario A (the constant model), the effective population size was constant at N1 from the present to the past.

In scenario B (the decline model), the effective population size changed from Na to N1 at t, and Na was larger than N1.

In scenario C (the expansion model), the effective population size changed from Na to N1 at t, and Na was smaller than N1.

In scenario D (the isolation and constant model), the populations were isolated, and the effective population size was constant at N1 from the present to the past.

In scenario E (the isolation and decline model), the populations were isolated, the effective population size changed from Na to N1 at t, and Na was larger than N1.

In scenario F (the isolation and expansion model), the populations were isolated, the effective population size changed from Na to N1 at t, and Na was smaller than N1.

For all analyses, the reference table was built with 1,000,000 simulated datasets per scenario using the following summary statistics: one-sample statistics for the number of haplotypes, Tajima's D, the mean number of pairwise differences, the variance of pairwise differences, and the number of segregating sites; and two-sample statistics for the mean of within-sample pairwise differences, the mean of between-sample pairwise differences, the number of segregating sites, and F_{ST} between samples. The posterior probabilities were compared by logistic regression. Additionally, the DIYABC program was used to estimate the population size of the ancestral populations of each species or metapopulation.

Migrations

Population genetic connectivity was assessed using the Bayesian MCMC method implemented in MIGRATE-N 4.4.3 (Beerli, 2016). MIGRATE-N calculates the mutation-scaled population size ($\theta = 2N_e\mu$ for haploid mtDNA) and immigration rate ($M = m/\mu$) for each area. Within *T. japonicus*, all sampling populations were separated into three metapopulations based on three oceanographic areas: the YS, ECS, and SCS. Four models of dispersal were first evaluated:

M1 is a full migration model with three population sizes and six immigration rates.

M2 is a source–sink model with three population sizes and three directional north-to-south immigration rates.

M3 is a source–sink model with three population sizes and three directional south-to-north immigration rates.

M4 is an island model where all areas share a single mean estimate of θ and exchange genes with all other areas at the same mean rate.

The models were ranked by log Bayes factors (LBFs), which compare the marginal likelihoods of models calculated using the

thermodynamic integration method. The most useful information is found in the model ranked first. The effective number of immigrants per generation was calculated for haploid data with female transmission following the equation $Nm = \theta \times M$. The MIGRATE-N program was also used to estimate the emigration and immigration of each population to better understand migration among populations. In these analyses, we ignored some populations that included too few samples, for example, population ZJ of *T. nanhaiensis*, population BH of *T. brevis*, and populations ST, ZJ, and WC of *T. japonicus* (**Table 1**). Finally, to examine whether the migrations of *T. japonicus* corresponded to feeding, our study also checked whether the stomach was empty and estimated the ratio of empty stomachs in each population.

RESULTS

Species Identification

A total of 1,224 hairtail fish were collected from 17 fishing ports along the China Seas (**Figure 1A**). Species were first identified by morphology. Two species groups were recognized: the *T. lepturus* complex, which has an anal opening positioned vertically at the 38th to 41st dorsal fin rays, and the *T. russelli* complex, which has an anal opening positioned vertically at the 34th to 35th dorsal fin rays (**Table 2**) (Burhanuddin et al., 2002). Within the *T. lepturus* complex, *T. japonicus* has a longer tail, and *T. lepturus* has a whitish dorsal fin when fresh; in contrast, *T. nanhaiensis* has a yellowish-green dorsal fin (Hsu et al., 2009); the frontal bone of *T. nanhaiensis* is very smooth, the frontal bone of *T. japonicus* is slightly inverted, and the frontal bone of *T. lepturus* is obviously inverted and bulges in the upper part of the orbit and is accompanied by indentation (**Figures S1, S2**; Yi et al., 2022). A total of 1,551 bp of the *COI* gene was sequenced. The nucleotide sequences were A+T rich (53.3%). To identify species, these sequences were analyzed by phylogenetic analysis and BLAST of the National Center for Biotechnology Information (NCBI, https://www.ncbi.nlm.nih.gov). The neighbor-joining (NJ) tree showed that these 1,224 *COI* sequences in the China Seas fell into three phylogroups (**Figure 1B**). Compared with the sequences in GenBank, these three phylogroups were identified as three species belonging to two species complexes: *T. nanhaiensis* and *T. japonicus* in the *T. lepturus* complex and *T. brevis* in the *T. russelli* complex. *Trichiurus nanhaiensis* and *T. brevis* are found only in the SCS, and the China Seas harbor *T. japonicus* (**Figure 1A**; **Table 1**).

Population Genetic Diversity and Structure

In total, 127 *COI* haplotypes from 203 specimens of *T. brevis* were sampled from six populations in the SCS (**Figure 1A**; **Table 1**). Among the 127 haplotypes, ten were shared by two or more populations. Population SY had the most shared haplotypes (**Table 1**). The most widespread haplotype was distributed among all six populations. According to N_{ST} (0.099) and G_{ST} (0.031), *T. brevis* displayed no significant phylogeographic structure or population differentiation (**Table 3**).

In total, 66 *COI* haplotypes from 119 specimens of *T. nanhaiensis* were sampled from three populations in the SCS (**Figure 1A**; **Table 1**). Although the sample size and the number of haplotypes of *T. nanhaiensis* were smaller than those of *T. brevis*, the nucleotide diversity (θ_π) was larger than that of *T. brevis* (**Table 1**). According to N_{ST} (0.149) and G_{ST} (0.038), *T. nanhaiensis* also displayed no significant phylogeographic structure or population differentiation (**Table 3**). Among the 66 haplotypes, only six were shared by two or more populations. ST and SZ populations shared the most haplotypes (five shared haplotypes).

In total, 521 *COI* haplotypes from 902 specimens of *T. japonicus* were sampled from 16 populations in the YS, ECS, and SCS (**Figure 1A**; **Table 1**). Among the 17 sampling populations, only SZ did not contain *T. japonicus*. The haplotype and nucleotide diversities of *T. japonicus* were larger than those of the other species (**Table 1**). Among the 521 haplotypes, 96 were shared by two or more populations. Population QD in the YS had the most private haplotypes, while population ZS in the ECS had the most shared haplotypes (**Table 1**). The northernmost population (DD) and the southernmost population (SY) had nine shared haplotypes. Two shared haplotypes were distributed widely in twelve and fourteen populations. The populations in the YS, ECS, and SCS had 85, 73, and 45 shared haplotypes, respectively. A total of 60, 39, and 32 haplotypes were shared by the YS and ECS, YS and SCS, and ECS and SCS, respectively. There were 26 haplotypes distributed in the China Seas. According to N_{ST} (0.000) and G_{ST} (0.002), *T. japonicus* displayed no phylogeographic structure or population differentiation (**Table 3**).

Population Demography and History

The significant negative values of Tajima's D and Fu's F_S supported a population expansion model for these three species (**Table 3**). The results of the mismatch distribution analysis showed that *T. japonicus*, *T. nanhaiensis*, and *T. brevis* all underwent population expansions, although the distributions

TABLE 2 | The identification keys of four *Trichiurus* species in Northwest Pacific.

1a. anal opening positioned vertically at the 38th to 41st dorsal fin rays.	*T. brevis*
1b. an anal opening positioned vertically at the 34th to 35th dorsal fin rays.	2
2a. whitish dorsal fin when fresh, and inverted frontal bone	3
2b. yellowish-green dorsal fin, and smooth frontal bone.	*T. nanhaiensis*
3a. longer tail (total length/preanal length), stouter head (head length/head depth), and slightly inverted frontal bone	*T. japonicus*
3b. shorter tail, slenderer head, and obviously inverted and bulges in the upper part of the orbit.	*T. lepturus*

*The photographs of these four Trichiurus species in **Figures S1, S2**.*

TABLE 3 | Results of dynamic tests and molecular clock analyses for *T. japonicus*, *T. nanhaiensis* and *T. brevis*.

Species	Tajima's D	Fu's Fs	SSD	Rg	R2	T_{MRCA} (95% CI)	N_{ST}	G_{ST}
T. japonicus	−2.616 (<0.001)	−7.233 (<0.02)	0.002 (0.570)	0.002 (0.970)	0.009	8.419 (6.742–10.118)	0.000	0.002
YS	−2.608 (<0.001)	−7.087 (<0.02)	0.002 (0.620)	0.002 (0.960)	0.012	4.863 (3.780–5.983)	0.002	0.001
ECS	−2.506 (<0.001)	−5.860 (<0.02)	0.002 (0.460)	0.002 (0.910)	0.016	4.305 (3.328–5.326)	0.004	0.000
SCS	−2.566 (<0.001)	−6.137 (<0.02)	0.003 (0.540)	0.002 (0.970)	0.021	8.145 (6.378–9.931)	0.000	0.008
T. nanhaiensis	−2.466 (<0.001)	−5.951 (<0.02)	0.002 (0.380)	0.010 (0.690)	0.022	1.485 (0.814–2.209)	0.149	0.038
T. brevis	−2.760 (<0.001)	−6.843 (<0.02)	0.001 (0.710)	0.012 (0.760)	0.013	3.988 (2.809–5.233)	0.099	0.031

The Tajima's D, Fu's F_S and mismatch distributions indices [i.e., sum of squared deviations from the sudden expansion model (SSD), raggedness index (Rg), and Ramos-Onsins and Rozas (R2)] are reported. The corresponding P-values are given in brackets. The time to the most recent common ancestor (T_{MRCA}) and two genetic differentiation indices (G_{ST} and N_{ST}) are also reported.

of pairwise differences seemed bimodal (**Figure 2**; **Table 3**). The BSPs showed that all species displayed population expansion at approximately 0.2–0.4 mya (**Figure 3A**). *Trichiurus japonicus* first slightly expanded at approximately 3.0 mya (data not shown); its population size was stable at 3.0–0.4 mya, and then it expanded again. At approximately 0.25 mya, the population size declined, and then it expanded again to 0.22 mya. Finally, at approximately 0.08 mya, the rate of population expansion declined (**Figure 3A**). *Trichiurus nanhaiensis* and *T. brevis* displayed a similar pattern. The populations of these two species both expanded at 0.20 and 0.24 mya, and the rate of population expansion declined at 0.15 and 0.18 mya (**Figure 3A**). Additionally, the population size of *T. nanhaiensis* has declined recently (**Figure 3A**).

Assigning the populations of *T. japonicus* to three metapopulations, YS, ECS, and SCS, the significant negative values of Tajima's D and Fu's F_S supported a population expansion model for these three metapopulations (**Table 3**). The results of the mismatch distribution analysis indicated a population expansion, and the distributions of pairwise differences seemed bimodal (**Figure 2**; **Table 3**). The patterns shown in the BSP among these three seas were slightly different, but still showed similarities (**Figure 3B**). The population underwent two expansion events. First, the population sizes in the YS, ECS, and SCS all expanded by 0.50 mya. Second, the population sizes in the YS, ECS, and SCS all expanded by 0.15–0.23 mya. Finally, the rate of population expansion in the YS and

ECS declined by 0.15 and 0.07 mya, respectively, but the rate in the SCS did not decline (**Figure 3B**). Additionally, before the second population expansion event, the YS suffered from declining pattern.

The results of a BEAST analysis suggested that the times to coalescence for *T. japonicus*, *T. nanhaiensis*, and *T. brevis* were sometime in the Late Miocene (T_{MRCA} = 8.419), Middle Pleistocene (T_{MRCA} = 1.485), and Middle Pliocene (T_{MRCA} = 3.988) (**Table 3**). The times to coalescence for the three metapopulations of *T. japonicus* were 4.863 (YS), 4.305 (ECS), and 8.145 (SCS).

The DIYABC results differed among these three species. In *T. nanhaiensis*, the highest posterior probability was found for the isolation and constant scenario (Scenario D). Its posterior probability (0.8908, 95% CI: 0.6205–1.0000) was higher than that of other scenarios (**Table 4**). In *T. brevis*, the highest posterior probability was also found for Scenario D. Its posterior probability was the highest (0.9976, 95% CI: 0.9791–1.0000). In *T. japonicus*, the highest posterior probability was found for the isolation and expansion scenario (Scenario F). Its posterior probability was the highest (1.0000, 95% CI: 0.9999–1.0000) (**Table 4**). In metapopulations of *T. japonicus*, the YS and ECS displayed the highest posterior probabilities for the isolation and constant scenarios (Scenario D, 1.0000 and 0.9931, respectively), and the highest posterior probability in the SCS was observed for the isolation and decline scenario (Scenario E; 0.9992, 0.9947–1.000; **Table 4**).
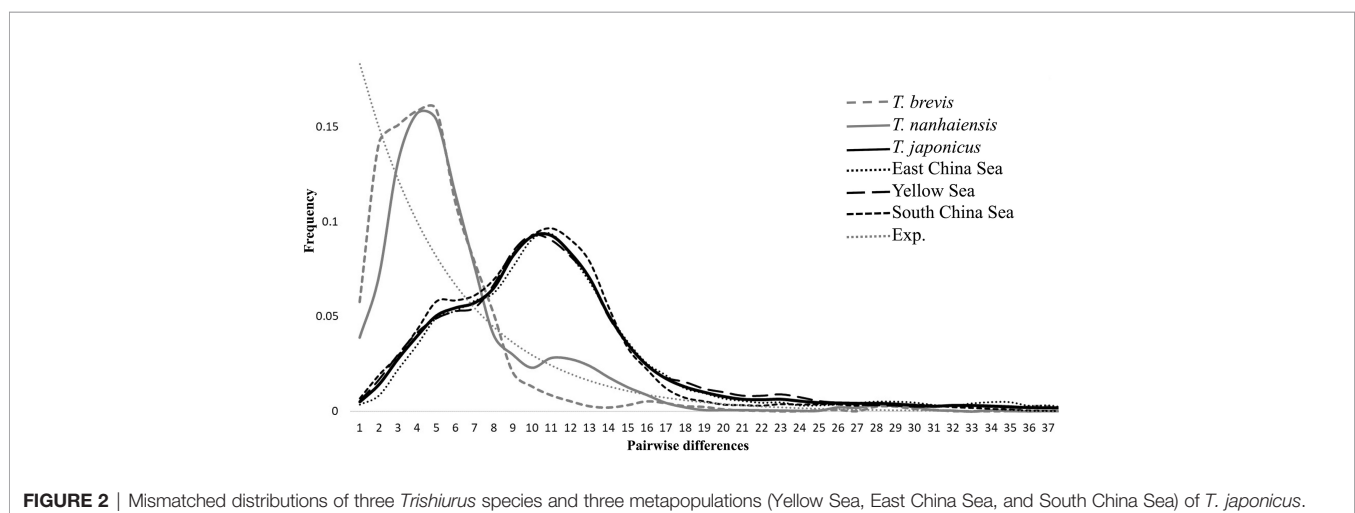
FIGURE 2 | Mismatched distributions of three *Trishiurus* species and three metapopulations (Yellow Sea, East China Sea, and South China Sea) of *T. japonicus*.
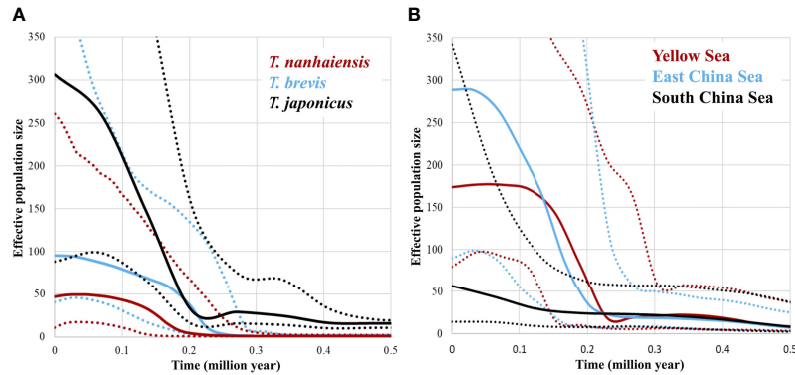
FIGURE 3 | Bayesian skyline plots of the effective population sizes through time in **(A)** *Trichiurus japonicus*, *T. nanhaiensis*, and *T. brevis*, and **(B)** three metapopulations (Yellow Sea, East China Sea, and South China Sea) of *T. japonicus*.

Population Genetic Connectivity

Migration estimates suggest that *T. japonicus* complies with a full migration model among the China Seas (M1; **Figure 4A**). M1 had the lowest log marginal likelihood of the four gene flow models tested (LBF = 0.00). Migrations among populations were also estimated (**Table S1**). The results of the regression analysis displayed no significant relationship between immigration and emigration in each population (y = 0.1186x + 6.2647, R^2 = 0.0064, where x = emigration and y = immigration; **Figure 4B**). In each population, populations WZ, ZS, and SY had the most immigration, and populations WH, ZS, and ND had the most emigrations (**Figure 5**). The values of emigration minus immigration in each population showed that most individuals did not stay in populations WH, ND, and YJ, and most individuals tended to stay in populations WZ, QZ, and SY (**Figure 5**).

In total, our study found that *T. japonicus* in the YS migrated southward to the ECS, and a few specimens migrated southward to the SCS (**Figure 6**; **Table S1**). Additionally, our study also found that some specimens of *T. japonicus* migrated from the SCS northward to the ECS (**Figure 6**). Furthermore, the results of the MIGRATE analysis showed that most specimens of *T. nanhaiensis* and *T. brevis* migrated northward from the SCS to

the Taiwan Strait (population ST), but few specimens migrated southward along the coast (**Figure 6**).

To determine whether the migrations of *T. japonicus* corresponded to feeding, our study also estimated the ratio of empty stomachs in each population (**Table 1**). Our study found that the empty stomach ratio in most populations is less than 0.50. The population DL in YS displayed the highest empty stomach ratio (0.82), and the population QZ in ECS displayed the lowest empty stomach ratio (0.17). The mean empty stomach ratios in the three seas were 0.52 (YS), 0.36 (ECS), and 0.53 (SCS). The regression analysis displayed no significant relationship between immigration and emigration and the ratio of empty stomachs (R^2 = 0.0067 and 0.0038, data not shown). These results might be because we only determined whether the stomach was empty in each specimen. Moreover, our study divided that data into two groups, with ratios of empty stomachs of more than 0.50 and less than 0.50. In the group with empty stomach ratios of less than 0.50, the regression analysis displayed no significant relationship between immigration and emigration and the ratio of empty stomachs (R^2 = 0.0934 and 0.0056, **Figure 7**). In the group with a ratio of empty stomachs greater than

TABLE 4 | Relative posterior probabilities for each scenario and their 95% confidence intervals in parentheses the based on the logistic estimate by DIYABC.

Species/ metapopulation	Scenario A constant	Scenario B decline	Scenario C expansion	Scenario D isolation-constant	Scenario E isolation-decline	Scenario F isolation-expansion
T. nanhaiensis	0.0137	0.0045	0.0000	**0.8908**	0.0906	0.0003
	(0.0000–0.0500)	(0.0000–0.0299)	(0.0000–0.0257)	(0.6205–1.0000)	(0.0000–0.3460)	(0.0000–0.0257)
T. brevis	0.0004	0.0020	0.0000	**0.9976**	0.0000	0.0000
	(0.0000–0.0026)	(0.0000–0.0197)	(0.0000–0.0000)	(0.9791–1.0000)	(0.0000–0.0000)	(0.0000–0.0000)
T. japonicus	0.0000	0.0000	0.0000	0.0000	0.0000	**1.0000**
	(0.0000–1.0000)	(0.0000–1.0000)	(0.0000–1.0000)	(0.0000–1.0000)	(0.0000–1.0000)	(0.9999–1.0000)
YS	0.0000	0.0000	0.0000	**1.0000**	0.0000	0.0000
	(0.0000–0.0000)	(0.0000–0.0000)	(0.0000–0.0000)	(1.0000–1.0000)	(0.0000–0.0000)	(0.0000–0.0000)
ECS	0.0065	0.0003	0.0000	**0.9931**	0.0000	0.0000
	(0.0000–0.0767)	(0.0000–0.0046)	(0.0000–0.0005)	(0.9212–1.0000)	(0.0000–0.0005)	(0.0000–0.0005)
SCS	0.0000	0.0000	0.0000	0.0008	**0.9992**	0.0000
	(0.0000–1.0000)	(0.0000–1.0000)	(0.0000–1.0000)	(0.0000–1.0000)	(0.9947–1.0000)	(0.0000–1.0000)

Bold indicated the highest probability.
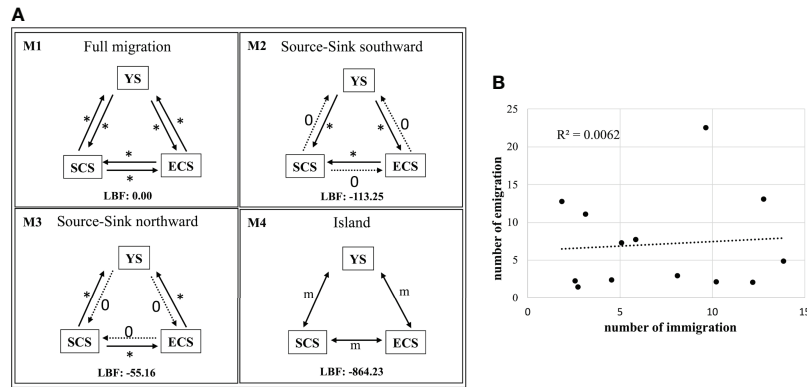
FIGURE 4 | The results of the analysis of the MIGRATE-N of *Trichiurus japonicus*. **(A)** Migration model diagrams. Arrows represent directions of gene flow among the three oceanographic groups, YS (Yellow Sea), ECS (East China Sea) and SCS (South China Sea). **(B)** The linear regression between total emigrations and total immigrations in each population inferred from model M1 provide0073 directions of gene flow (*Nem*). *, number of migrations.

0.50, the regression analysis displayed a slightly significant relationship between immigration and emigration and the ratio of empty stomachs (R^2 = 0.1182 and 0.3449, **Figure 7**). When our study estimated immigration, emigration, and the ratio of empty stomachs in three seas, the regression analysis displayed a strong significant relationship between immigration and emigration and the ratio of empty stomachs (R^2 = 0.5207 and 0.9710, data not shown), although the sample size was only three (YS, ECS, and SCS).

DISCUSSION

Species Habitat Characterization

A species is a necessary unit in all biological, ecological, and genetic studies. Clear species identification for fishery management purposes has been the subject of a major FAO program since the 1960s. However, the taxonomic status of the hairtail has not been resolved, especially within the genus *Trichiurus*. The species within the genus *Trichiurus* could be assigned to two groups: large-headed and short-tailed fishes (Hsu et al., 2009). The large-head group is also referred to as the

T. lepturus species complex. Hsu et al. (2009) found three species within this species complex: *T. japonicus*, *T. nanhaiensis*, and *T. lepturus*. *T. japonicus* was distributed along the continental shelves in the northeastern Pacific, especially in the seas around Japan and mainland China. *T. nanhaiensis* was primarily distributed in the SCS, and *T. lepturus* was distributed in the Pacific and Atlantic. According to Hsu et al. (2009), only *T. japonicus* and *T. nanhaiensis* were distributed along the coast of the Asian continent. The findings of this study (**Figure 1A**; **Table 1**) and He et al. (2014) supported these distribution patterns. Although *T. japonicus* is distributed throughout all the China Seas, it is much less abundant in the SCS. The findings of this study revealed that *T. brevis* is more abundant in the SCS than other *Trichiurus* species (**Figure 1A**; **Table 1**).

The sea temperature in the SCS is higher than that in the ECS and YS. Accordingly, our study suggests that these three *Trichiurus* species have different habitat preferences along the coast of China. *T. japonicus* prefers colder waters on the continental shelves, while *T. nanhaiensis* prefers warmer waters on continental slopes and *T. brevis* prefers warmer waters on the continental shelves. These results corresponded to the results of Hou et al. (2021). Hou et al. (2021) found that
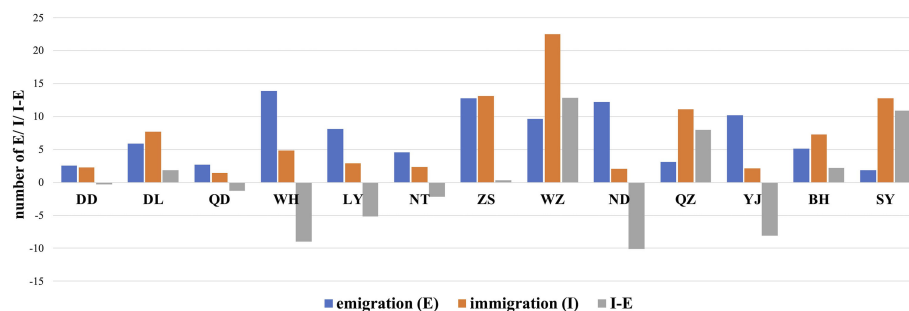
FIGURE 5 | The bar graphs indicated the total emigrations and immigrations, and the values of emigrations minus immigrations in each population of *Trichiurus japonicus*. See **Table 1** and **Figure 1** for the population names and locations.
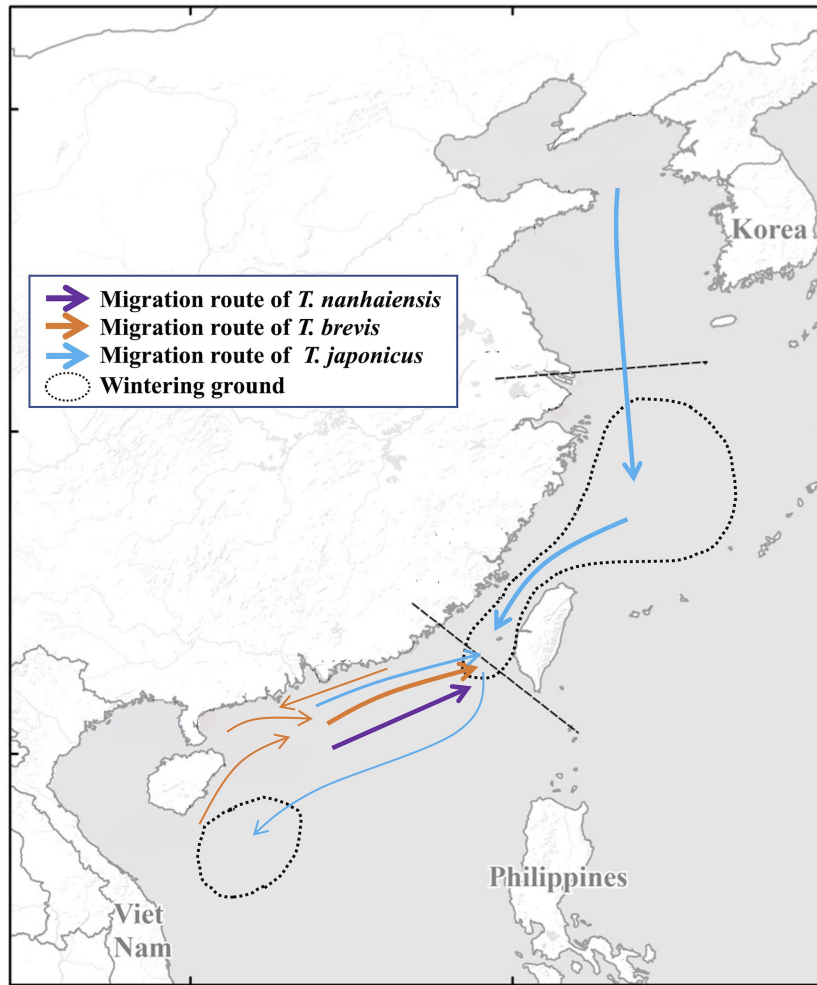
FIGURE 6 | A map showing the migration routes of the *Trichiurus* species and wintering grounds along the China Seas.

the spawning of *T. japonicus* occurs along the continental shelf, *T. nanhaiensis* occurs along the continental shelf to the slope, and *T. brevis* occurs in shallow water. Although our study found that *T. nanhaiensis* and *T. brevis* migrated from the SCS to the southern end of the Taiwan Strait (see below: *Migration for Feeding and Spawning*), the

Taiwan Strait is a barrier to the distribution patterns of other species (e.g., Liu et al., 2007; Xu et al., 2009; Liu et al., 2011; Hsu et al., 2021). The spatial and temporal distributions of *Trichiurus* species are determined by hydrological conditions, e.g., salinity and temperature (Hou et al., 2021).
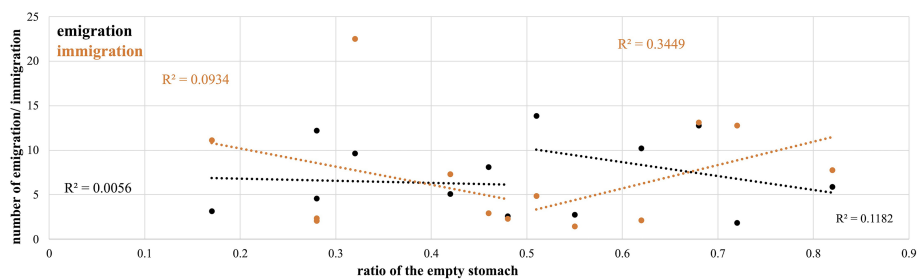
FIGURE 7 | The linear regression between emigrations and immigration and the ratio of the empty stomach in each *Trichiurus japonicus* population.

Genetic Diversity and Structure

Among these three *Trichiurus* species along the Chinese coastline, the genetic diversity (θ_π) of *T. japonicus* was higher than that of *T. nanhaiensis* and *T. brevis*, and the latter two species had similar genetic diversity (**Table 1**). However, the T_{MRCA} of *T. japonicus* was higher than that of *T. nanhaiensis* and *T. brevis*, and that of *T. brevis* was higher than that of *T. nanhaiensis* (**Table 3**). Genetic diversity did not correspond to the TMRCA values. Yi et al. (2021a) found that the size of the specimen distribution of a given species and its genetic diversity are positively related based on the family Apogonidae in the SCS. Our study found that *T. nanhaiensis* and *T. brevis* are found only in the SCS, and *T. japonicus* is found in all the China Seas (**Figure 1A**; **Table 1**). Thus, our study suggests that the genetic diversity and the size of the specimen distribution area have positive relationships.

The results of N_{ST} and G_{ST} showed that these three *Trichiurus* species lacked population structure (**Table 3**). The distribution of the shared haplotypes also suggested that gene flows among populations were frequent. However, our study found that the results of the mismatch distribution analysis showed that the distributions of pairwise differences in these three *Trichiurus* species seemed bimodal (**Figure 2**). Previous studies reported that the bimodal mismatch distribution reveals population divergences (Yan et al., 2020; Yi et al., 2021b). Some studies found that there were two spawning cohorts of *T. japonicus* in the ECS and SCS, from February–July and November–December (Sun et al., 2020a; Sun et al., 2020b). The results of the DIYABC analyses also showed that the populations of *Trichiurus* species met in isolation (**Table 4**).

Additionally, the results of the T_{MRCA} displayed a strange pattern (**Table 3**). The T_{MRCA} of the total of *T. japonicus* and that of the metapopulation in the SCS were close (8.419 and 8.15), but those in the metapopulations in the YS and ECS were 4.863 and 4.305, respectively. However, *T. japonicus* was mainly distributed in the YS and ECS, and the population sizes in the YS and ECS were higher than those in the SCS (**Figure 3B**). Our study suggests that during glaciations, YS and ECS were completely exposed, and the SCS became a refugium. Thus, the T_{MRCA} in the SCS and that of the total samples were similar and higher than those in the YS and ECS (**Table 3**). This result also implied that some populations of *T. japonicus* retreated to the SCS during glaciations and settled in interglacial periods. Thus, although our study found no significant genetic differentiation of these three *Trichiurus* species along the Chinese coastline because their swimming abilities were strong, we considered that *Trichiurus* species might have been differentiated in the China Seas and were shaped by landform changes during glaciations, as in other previous phylogeographic studies (e.g., Shen et al., 2011; Yang et al., 2017; Qu et al., 2018). Sea level and temperature fluctuations promoted differentiation in the Northwestern Pacific Ocean (Liu et al., 2006; Shen et al., 2011; Qu et al., 2018).

Migrations for Feeding and Spawning

Jaureguizar et al. (2004) proposed that the major aims of fish migrations are seasonal and reproductive. Sun et al. (2020a) also proposed that *T. japonicus* undergoes seasonal migration. Our study sampled specimens in the late fall and early winter. In this season, marine species might migrate southward, following warm waters through the China Coastal Current (**Figure 1**). Our study found that these three *Trichiurus* species generally did not migrate southward through the China Coastal Current (**Figures 1**, **6**). The migration pattern of *T. japonicus* was supported by the full migration model (**Figure 4A**). Regression analysis revealed no significant positive relationship between immigration and emigration in each population (y = 0.1186x + 6.2647, R^2 = 0.0064, where x = emigration and y = immigration; **Figure 4B**). These results might have resulted in their strong swimming abilities.

According to the migrations between populations, our study inferred the migration routes of *T. japonicus* and found that most specimens migrated from the YS southward to the ECS and SCS (**Figure 6**). Most specimens remain in the ECS, including the Taiwan Strait. Moreover, our study also found that some specimens migrated northward from the SCS to the Taiwan Strait. Our study also revealed that *T. nanhaiensis* and *T. brevis* migrated from the SCS to the Taiwan Strait (**Figure 6**). This region, south of the Yangtze River and north of the Taiwan Strait, has been recognized as the wintering ground of *T. japonicus* (Wang et al., 2011; Sun et al., 2020a; Sun et al., 2020b). In this region, the waters are formed by the Kuroshio Current and diluted Yangtze waters. The former current has high salinity and temperature, and the latter has low salinity and abundant nutrients (Chen et al., 2009). The branch of the Kuroshio Current flows from the east of the Philippines through the Bashi Channel into the Taiwan Strait. Moreover, Han et al. (2013) also found that nutrient transport from the ECS is a major source of support for winter primary production on the northeastern SCS shelf through the Taiwan Strait. Thus, there is more biomass in this area than in the surrounding areas. The northern wintering ground extended to the Taiwan Strait and northeastern SCS. Jaureguizar et al. (2004) suggest that both seasonal migrations and reproductive movements are affected by temporal structure. Chiang et al. (2002) also proposed that water temperature is a limiting factor for phytoplankton biomass density, and that carbon biomass increases in the warm season. Accordingly, our study suggests that these migrations of the *Trichiurus* species were shaped by feeding (**Figure 7**). Our study suggested that the ECS, including the Taiwan Strait, is a wintering ground for *T. japonicus*, and *T. nanhaiensis* and *T. brevis* winter in the northeastern SCS (**Figure 6**).

In addition to the wintering grounds in the ECS, including the Taiwan Strait, our study found that some specimens of *T. japonicus* remained in population SY (**Figure 5**). The water temperature in the SCS is higher than that in the YS and ECS. Hou et al. (2021) found that in late summer and early autumn, eggs of *T. japonicus* and *T. nanhaiensis* mainly occurred in the surface water mass of the SCS. Thus, our study suggests that population SY is a wintering and spawning ground for *T. japonicus* (**Figure 6**). These results also supported the results of the T_{MRCA} (**Table 3**). During the LGM, *T. japonicus* migrated from the YS and ECS to the SCS as a refugium, and some populations settled during the interglacial period. Accordingly,

our study suggests that the migrations of *Trichiurus* species are mainly associated with feeding and spawning preferences and that the behavior is shaped by oceanographic conditions (e.g., Han et al., 2013; Liu et al., 2020; Hou et al., 2021).

Demographic History in Different Samplings

Many studies of marine species have revealed a population expansion before or after the Last Glacial Maximum (pre-LGM or post-LGM; Delrieu-Trottin et al., 2017; Jenkins et al., 2018; Qu et al., 2018). Jenkins et al. (2018) also proposed that some species display stable population sizes pre- and post-LGM. Clark et al. (2009) identified the interval with LGM as between 0.027 and 0.019 mya. Our study found that these three *Trichiurus* species all showed a population expansion after the LGM (**Figure 3A**). Previous studies also displayed similar patterns (He et al., 2014; Lin et al., 2021). However, our results and those of He et al. (2014) displayed two different patterns. First, in the results of He et al. (2014), *T. japonicus* in the ECS experienced a genetic bottleneck, but in our results, *T. japonicus* in the YS experienced a genetic bottleneck, and that in the ECS did not (**Figure 3B**). Second, in the results of He et al. (2014), the population of *T. japonicus* in the SCS declined, but in our results, the population expanded (**Figure 3B**). Our study considered that these differences might have resulted from the sampling season. He et al. (2014) might have sampled in winter, while our study samples were collected in late fall and early winter. In winter, *T. japonicus* migrated from the YS to the ECS and SCS. Thus, the patterns in He et al. (2014) shifted from north to south.

Limits of the Bayesian Skyline Plot Analysis

The neutrality tests, mismatch distribution, and coalescent BSPs supported population expansion (**Table 3**; **Figures 2**, **3**), but the approximate Bayesian computational approaches supported population declines or remained constant (**Table 4**). The incongruent results between approximate Bayesian computational approaches (**Table 4**) and other demographic analyses (**Table 3**; **Figures 2**, **3**) might have resulted in a population differentiation (Heller et al., 2013; Yan et al., 2020; Yi et al., 2021b). Heller et al. (2013) proposed that the results of BSP analyses show false signals of population decline under biologically plausible combinations of population structure. Yan et al. (2020) and Yi et al. (2021b) also found that when populations met differentiation, the results of the BSP analyses displayed population expansion, but other analyses, e.g., mismatch distribution and Tajima's D test, did not support the population expansion. Furthermore, the BSPs revealed that the population sizes of three *Trichiurus* species and three metapopulations of *T. japonicus* all displayed population expansion after the LGM and experienced a genetic bottleneck during the LGM (**Figure 3**). However, our study did not find that during the last interglacial period, the population size was not higher than that during glaciation in BSP (**Figure 3**; He et al., 2014). In other words, the population size was stable in the glacial and the last interglacial periods. Grant et al. (2012) found that the BSPs of simulated sequences showed a flat demographic

curve before the LGM and suggested that the results of the BSP analyses lost the pre-LGM population history. Accordingly, our results also support limits in BSP analyses (Grant et al., 2012; Heller et al., 2013). Thus, the results of BSP analyses may need to be evaluated carefully.

Demography of *Trichiurus* Species

Our study suggests that the *Trichiurus* species underwent population differentiation due to landform changes during the Pliocene and Pleistocene glacial cycles, as in previous phylogeographic studies (Kizaki and Oshiro, 1980; Ota, 1994; Wang, 1999; Voris, 2000; Yang et al., 2017; Qu et al., 2018). The complex geological history might cause incorrect assessment in BSP analyses. However, our study did find evidence supporting the population history of *Trichiurus* species based on all the results.

Among the three *Trichiurus* species, the BSP results revealed that the population size of *T. nanhaiensis* was lower than that of the other two species, and only this species recently displayed population decline (**Figure 3A**). However, the genetic diversity of *T. nanhaiensis* was not lower than that of the other species (**Table 1**). Previous studies found that population differentiation could result in overestimated genetic diversity (Yan et al., 2020; Yi et al., 2021b). Our study found that the level of population differentiation of *T. nanhaiensis* was higher than that of the other two species (N_{ST}; **Table 3**). Thus, our study showed that the BSP results and genetic diversity in *T. nanhaiensis* might be overestimated, and the population size of *T. nanhaiensis* seriously declined (**Figure 3A**). Our study also found that people ate *T. nanhaiensis* more frequently in the South Sea (our observations) because this species is meatier than *T. japonicus* and *T. brevis*.

The BSP results also revealed different patterns among the three metapopulations of *T. japonicus* (**Figure 3B**). The estimated population size in the ECS was the highest, and that in the SCS was the lowest. These results corresponded to the annual marine capture fishery production of China (Kang et al., 2018). Thus, our study suggests that *T. japonicus* can be used as an indicator organism to monitor fishery resources in the China Seas. The ECS is the largest marginal sea in the northwestern Pacific, and there are more nutrient sources here than in other areas, including those from the Kuroshio Current and Yangtze River runoff (Chiang et al., 2002). Additionally, in our sampling season, *T. japonicus* migrated from the YS to the ECS as a wintering ground. Thus, the population size in ECS was higher. The YS is a semi-enclosed body of water, but the coastline is heavily populated, urbanized, and industrialized. Ji et al. (2019) proposed that the largehead hairtail in YS, including the Bohai Sea, experienced overexploitation. Moreover, in our sampling season, the populations in the YS migrated southward. Thus, the YS metapopulation declined significantly (**Figure 3B**). Furthermore, the population size in the SCS increased according to the BSP results (**Figure 3B**). Liu (2013) proposed that among the marginal seas of China, the South China Sea has the highest biodiversity. Our study also inferred a wintering and spawning ground in the SCS, and some populations migrated from the YS and ECS southward to the SCS (**Figure 6**). As the BSP analyses have limitations, the BSP results would

display false signals of population decline under combinations of population structure. Thus, although the BSP results showed population growth in the SCS, the SCS population size was the lowest (**Figure 3B**). Kang et al. (2018) and Du et al. (2020) found that resources experienced a decline in catch per unit effort (CPUE), the annual catch in the YS decreased after 2008, the annual increments declined in the ECS and SCS, and a rapid decrease in the annual capture of the SCS began in 2018. Thus, our study suggests that policies are needed for the resource management of *Trichiurus* species.

CONCLUSION

Our study found that the three *Trichiurus* species studied have different habitat preferences along the coast of China. *T. japonicus* prefer colder waters on continental shelves, while *T. nanhaiensis* prefer warmer waters on continental slopes and *T. brevis* prefer warmer waters on the continental shelves. Our study showed that the distribution and intraspecific genetic structure of *Trichiurus* species were controlled by feeding and spawning, and the behavior might be shaped by environmental factors (Liu et al., 2020; Hou et al., 2021). Wang H. Y. et al., (2017) proposed temporal changes in hairtail composition. Moreover, our study suggested that the different results in the present study and those of He et al. (2014) were due to the different sampling seasons. Berger-Tal and Saltz (2019) proposed that movement and habitat selection are linked to the distribution of animals in space and time, and changes in movement patterns impact on the ecosystem. As a result, while habitat protection is an important step in the preserving biodiversity, our study suggests that, in addition to *in situ* conservation in two wintering and spawning grounds, an annual catch limit policy is required. These results will provide suggestions for protecting fish resources and habitat restoration.

DATA AVAILABILITY STATEMENT

All nucleotide sequences were deposited in GenBank under accessions MZ959870–MZ959999, MZ960057–MZ960127, and OK053821–OK054341.

ETHICS STATEMENT

All animal experiments were carried out in accordance with the guidelines and approval of the Animal Research and Ethics Committee of the College of Fisheries, Guangdong Ocean University (permissions, B20200722-01).

AUTHOR CONTRIBUTIONS

Y-RY and H-DL designed the study. K-CH and M-RY analyzed most of the data and wrote the initial draft of the paper. Y-RY, H-DL, and BK discussed and revised the manuscript. SG and Z-SL performed the experiments. X-BH collected samples and the data. All authors listed have made a substantial, direct, and intellectual contribution to the work and approved it for publication.

FUNDING

ACKNOWLEDGMENTS

SUPPLEMENTARY MATERIAL

The Supplementary Material for this article can be found online at: https://www.frontiersin.org/articles/10.3389/fmars.2022.875042/full#supplementary-material

REFERENCES

Beerli, P. (2016) *MIGRATE-N 4.4.3*. Available at: https://peterbeerli.com/migrate/tutorials.html.

Berger-Tal, O., and Saltz, D. (2019). Invisible Barriers: Anthropogenic Impacts on Inter- and Intra-Specific Interactions as Drivers of Landscape-Independent Fragmentation. *Phil. Trans. R. Soc. B.* 374, 20180049. doi: 10.1098/rstb.2018b0049

Burhanuddin, A. I., Iwatsuki, Y., Yoshino, T., and Kimura, S. (2002). Small and Valid Species of *Trichiurus Brevis* Wang and You 1992 and *T. Russelli* Dutt and Thankam 1966, Defined as the "*T. Russelli* Complex" (Perciformes: Trichiuridae). *Ichthyol. Res.* 49, 211–223. doi: 10.1007/s102280200030

Chakraborty, A., Aranishi, F., and Iwatsuki, Y. (2006). Genetic Differences Among Three Species of the Genus *Trichiurus* (Perciformes: Trichiuridae) Based on Mitochondrial DNA Analysis. *Ichthyol. Res.* 53, 93–96. doi: 10.1007/s10228-005-0313-3

Chen, C. C., Shiah, F. K., Chaing, K., Gong, G. C., and Kemp, W. M. (2009). Effects of the Changjiang (Yangtze) River Discharge on Planktonic Community Respiration in the East China Sea. *J. Geophys. Res.* 114, C03005. doi: 10.1029/2008JC004891

Chiang, K. P., Kuo, M. C., Chang, J., Wang, R. H., and Gong, G. C. (2002). Spatial and Temporal Variation of the *Synechococcus* Population in the East China Sea and Its Contribution to Phytoplankton Biomass. *Cont. Shelf Res.* 22, 3–13. doi: 10.1016/S0278-4343(01)00067-X

Chiu, Y. W., Bor, H., Kuo, P. H., Hsu, K. C., Tan, M. S., Wang, W. K., et al. (2017). Origins of *Semisulcospira Libertina* (Gastropoda: Semisulcospiridae) in Taiwan. *Mitochondrial DNA Part A* 28, 518–525. doi: 10.3109/24701394. 2016.1149823

Clark, P. U., Dyke, A. S., Shakun, J. D., Carlson, A. E., Clark, J., Wohlfarth, B., et al. (2009). The Last Glacial Maximum. *Science* 325, 710–714. doi: 10.1126/ science.1172873

Cornuet, J. M., Pudlo, P., Veyssier, J., Dehne-Garcia, A., Gautier, M., Leblois, R., et al. (2014). DIYABC V2.0: A Software to Make Approximate Bayesian Computation Inferences About Population History Using Single Nucleotide Polymorphism, DNA Sequence and Microsatellite Data. *Bioinformatics* 30, 1187–1189. doi: 10.1093/bioinformatics/btt763

Darriba, D., Taboada, G. L., Doallo, R., and Posada, D. (2012). Jmodeltest 2: More Models, New Heuristics and Parallel Computing. *Nat. Methods* 9, 772–772. doi: 10.1038/nmeth.2109

Delrieu-Trottin, E., Mona, S., Maynard, J., Neglia, V., Veuille, M., and Planes, S. (2017). Population Expansions Dominate Demographic Histories of Endemic and Widespread Pacific Reef Fishes. *Sci. Rep.* 7, 40519. doi: 10.1038/srep40519

Drummond, A. J., Rambau, A., and Suchard, M. (2013) *BEAST 1.8.0.* Available at: http://beast.bio.ed.ac.uk (Accessed March 26, 2021).

Du, P., Chen, Q. Z., Yan, Y. R., Ye, W. J., Li, S. L., and Yu, C. G. (2020). Advances in the *Trichiurus Lepturus* Changes and Habitat Driving Factors in the East China Sea. *J. Guangdong Ocean Univ.* 40, 126–132. doi: 10.3969/j.issn.1673-9159.2020.01.017

Eschmeyer, W. N. (2014). *Catalog of Fishes* (San Francisco, CA: California Academy of Science).

FAO (2012). *Yearbook 2010* (Rome, Italy: Fishery and Aquaculture Statistics).

FAO (2016). *Yearbook 2014* (Rome, Italy: Fishery and Aquaculture Statistics).

Froese, R., and Pauly, D. (2021). *FishBase* (World Wide Web Electronic Publication). Available at: http://www.fishbase.org.

Fu, Y. X. (1997). Statistical Tests of Neutrality of Mutations Against Population Growth, Hitchhiking and Background Selection. *Genetics* 147, 915–925. doi: 10.1093/genetics/147.2.915

Golani, D., and Fricke, R. (2018). Checklist of the Red Sea Fishes With Delineation of the Gulf of Suez, Gulf of Aqaba, Endemism and Lessepsian Migrants. *Zootaxa* 4509, 1–215. doi: 10.11646/zootaxa.4509.1.1

Grant, W. S., Liu, M., Gao, T., and Yanagimoto, T. (2012). Limits of Besesian Skyline Plot Analysis of mtDNA Sequences to Infer Historical Demographies in Pacific Herring (and Other Species). *Mol. Phylogenet. Evol.* 65, 203–212. doi: 10.1016/j.ympev.2012.06.006

Gu, S., Yi, M. R., He, X. B., Lin, P. S., Liu, W. H., Luo, Z. S., et al. (2021). Genetic Diversity and Population Structure of Cutlassfish (*Lepturacanthus Savala*) Along the Coast of Mainland China, as Inferred by Mitochondrial and Microsatellite DNA Markers. *Reg. Stud. Mar. Sci.* 43, 101702. doi: 10.1016/ j.rsma.2021.101702

Hall, T. A. (1999). BioEdit: A User-Friendly Biological Sequence Alignment Editor and Analysis Program for Windows 95/98/NT. *Nucleic Acids Symp.* 41, 95–98. doi: 10.1017/CB9780511790492.007

Han, A. Q., Dai, M. H., Gan, J. P., Kao, S. J., Zhao, X. Z., Jan, S., et al. (2013). Inter-Shelf Nutrient Transport From the East China Sea as a Major Nutrient Source Supporting Winter Primary Production on the Northeast South China Sea Shelf. *Biogeosciences* 10, 8159–8170. doi: 10.5194/bg-10-8159-2013

Han, C. C., Hsu, K. C., Fang, L. S., Chang, I. M., and Lin, H. D. (2019). Geographical and Temporal Origins of *Neocaridina* Species (Decapoda: Caridea: Atyidae) in Taiwan. *BMC Genet.* 20, 86. doi: 10.1186/s12863-019-0788-y

Hebert, P. D. N., Stoeckle, M. Y., Zemlak, T. S., and Francis, C. M. (2004). Identification of Birds Through DNA Barcodes. *PloS Biol.* 2, 1657–1663. doi: 10.1371/journal.pbio.0020312

Heller, R., Chikhi, L., and Siegismund, H. R. (2013). The Confounding Effect of Population Structure on Bayesian Skyline Plot Inferences of Demographic History. *PloS One* 8, e62992. doi: 10.1371/journal.pone.0062992

He, L., Mukai, T., Hou, C. K., Ma, Q., and Zhang, J. (2015). Biogeographical Role of the Kuroshio Current in the Amphibious Mudskipper *Periophthalmus Modestus* Indicated by Mitochondrial DNA Data. *Sci. Rep.* 5, 15645. doi: 10.1038/srep15645

He, L., Zhang, A., Weese, D., Li, S., Li, J., and Zhang, J. (2014). Demographic Response of Cutlassfish (*Trichiurus Japonicus* and *T. Nanhaiensis*) to Fluctuating Palaeo-Climate and Regional Oceanographic Conditions in the China Seas. *Sci. Rep.* 4, 6380. doi: 10.1038/srep06380

Hou, G., Xu, Y., Chen, Z., Zhang, K., Huang, W., Wang, J., et al. (2021). Identification of Eggs and Spawning Zines of Hairtail Fishes *Trichiurus* (Pisces: Trichiuridae) in Northern South China Sea, Using DNA Barcoding. *Front. Environ. Sci.* 9, 703029. doi: 10.1007/s00343-011-0004-z

Hsu, K. C., Shih, N. T., Ni, I. H., and Shao, K. T. (2009). Speciation and Population Structure of Three *Trichiurus* Species Based on Mitochondrial DNA. *Zool. Stud.* 48, 835–849.

Hsu, K. C., Wu, H. J., Kuo, P. H., and Chiu, Y. W. (2021). Genetic Diversity of *Cyclina Sinensis* (Veneridae): Resource Management in Taiwan. *Taiwania* 66, 165–173. doi: 10.6165/tai.2021.66.165

Jaureguizar, A. J., Menni, R., Guerrero, R. , and Lasta, C. (2004). Environmental Factors Structuring Fish Communities of the RíIo De La Plata Estuary. *Fish. Res.* 66, 195–211. doi: 10.1016/S0165-7836(03)00200-5

Jenkins, T. L., Castilho, R., and Stevens, J. R. (2018). Meta-Analysis of Northeast Atlantic Marine Taxa Shows Contrasting Phylogeographic Patterns Following Post-LGM Expansions. *PeerJ* 6, e5684. doi: 10.7717/peerj.5684

Ji, Y., Liu, Q., Liao, B., Zhang, Q., and Han, Y. (2019). Estimating Biological Reference Points for Largehead Hairtail (*Trichiurus Lepturus*) Fishery in the Yellow Sea and Bohai Sea. *Acta Oceanol. Sin.* 38, 20–26. doi: 10.1007/s13131-019-1343-4

Jukes, T. H., and Cantor, C. R. (1969). "Evolution of Protein Molecules," in *Mammalian Protein Metabolism*. Ed. H. N. Monro (New York, NY: Academic Press), 21–132.

Kang, B., Liu, M., Huang, X. X., Li, J., Yan, Y. R., Han, C. C., et al. (2018). Fisheries in Chinese Seas: What Can We Learn From Controversial Official Fisheries Statistics? *Rev. Fish Biol. Fisheries* 28, 503–519. doi: 10.1007/s11160-018-9518-1

Kizaki, K., and Oshiro, I. (1980). *The Origin of the Ryukyu Islands. Natural History of the Ryukyus*. Ed. K. Kizaki (Tokyo: Tsukiji-shokan), 8–37.

Kumar, S., Steecher, G., Li, M., Knyaz, C., and Tamura, K. (2018). MEGA X: Molecular Evolutionary Genetics Analysis Across Computing Platforms. *Mol. Biol. Evol.* 35, 1547–1549. doi: 10.1093/molbev/msy096

Lee, S. C., Chang, K. H., Wu, W. L., and Yang, H. C. (1977). Formosan Ribbonfishes (Perciformes, Trichiuridae). *Bull. Instit. Zool.* 16, 77–84.

Liao, T. Y., Lu, P. L., Yu, Y. H., Huang, W. C., Shiao, J. H., Lin, H. D., et al. (2021). Amphidromous But Endemic: Population Connectivity of *Rhinogobius Gigas* (Teleostei: Gobioidei). *PloS One* 16, e0246406. doi: 10.1371/journal.pone. 0246406

Librado, P., and Rozas, J. (2009). DnaSP V5: A Software for Comprehensive Analysis of DNA Polymorphism Data. *Bioinformatics* 25, 1451–1452. doi: 10.1093/bioinformatics/btp187

Lin, H. C., Tsai, C. J., and Wang, H. Y. (2021). Variation in Global Distribution, Population Structures, and Demographic History for Four *Trichiurus* Cutlassfishes. *PeerJ* 9, e12639. doi: 10.7717/peerj.12639

Liu, J. Y. (2013). Status of Marine Biodiversity of the China Seas. *PloS One* 8, e50719. doi: 10.1371/journal.pone.0050719

Liu, J., Gao, T. X., Wu, S., and Zhang, Y. A. P. (2007). Pleistocene Isolation in the Northwestern Pacific Marginal Seas and Limited Dispersal in a Marine Fish, *Chelon Haematocheilus* (Temminck & Schlege). *Mol. Ecol.* 16, 275–288. doi: 10.1111/j1365-294X.2006.03140.x

Liu, J. X., Gao, T. X., Yokogawa, K., and Zhang, Y. P. (2006). Differential Population Structuring and Demographic History of Two Closely Related Fish Species, Japanese Sea Bass (*Lateolabrax Japonicus*) and Spotted Sea Bass (*Lateolabrax Maculatus*) in Northwestern Pacific. *Mol. Phylogenet. Evol.* 39, 799–811. doi: 10.1016/j.ympev.2006.01.009

Liu, J., Li, Q., Kong, L. F., and Zheng, X. D. (2011). Cryptic Diversity in the Pen Shell *Atrina Pectinata* (Bivalvia: Pinnidae): High Divergence and

Hybridization Revealed by Molecular and Morphological Data. *Mol. Ecol.* 20, 4332–4345. doi: 10.1111/j.1365-294X.2011.05275.x

Liu, S., Liu, Y., Alabia, I. D., Tian, Y., Ye, Z., Yu, H., et al. (2020). Impact of Climate Change on Wintering Ground of Japanese Anchovy (*Engraulis Japonicus*) Using Marine Geospatial Statistics. *Front. Mar. Sci.* 7. doi: 10.3389/fmars.2020.00604

Nakabo, T. (2000). *Fishes of Japan With Pictorial Keys to the Species. 2nd* (Tokyo: Tokai Univ. Press).

Nakamura, I., and Parin, N. V. (1993). An Annotated and Illustrated Catalogue of the Snakemackerels, Snoeks, Escolars, Gemfishes, Sackfishes, Domine, Oilfish, Cutlassfishes, Scabbardfishes, Hairtails, and Frostfishes Known to Date. *FAO Fish. Syn.* 125, 200.

Nakamura, I., and Parin, N. V. (2001). Families Gempylidae, Trichiuridae. In: Carpenter & Niem 2001. Species Identification Guide for Fishery Purposes. The Living Marine Resources of the Western Central Pacific. Bony Fishes Part 4 (Labridae to Latimeriidae), Estuarine Crocodiles, Sea Turtles, Sea Snakes and Marine Mammals. *FAO Rome.* v. 6: iii–v.

Nei, M., and Tajima, F. (1983). Maximum Likelihood Estimation of the Number of Nucleotide Substitutions From Restriction Sites Data. *Genetics* 105, 207–217. doi: 10.1093/genetics/105.1.207

Nelson, J. S. (1994). *Fishes of the World, 3rd Edn* (New York: J Wily).

Ota, H. (1994). *Biogeographical Characteristics of Terrestrial Vertebrates of the Ryukyu Archipelago.* In: Search of Origins of Okinawan Culture (Executive Committee International Symposium on Okinawan Studies, Ed.). Naha: Bunshinlnsatsu. 460–464.

Picq, S., Alda, F., Krahe, R., and Bermingham, E. (2014). Miocene and Pliocene Colonization of the Central American Isthmus by the Weakly Electric Fish *Brachyhypopomus Occidentalis* (Hypopomidae, Gymnotiformes). *J. Biogeogr.* 41, 1520–1532. doi: 10.1111/jbi.12309

Pons, O., and Petit, R. J. (1996). Measuring and Testing Genetic Differentiation With Ordered vs. Unordered Alleles. *Genetics* 144, 1237–1245. doi: 10.1093/genetics/144.3.1237

Qu, M., Tang, W., Liu, Q., Wang, D., and Ding, S. (2018). Genetic Diversity Within Grouper Species and a Method for Interspecific Hybrid Identification Using DNA Barcoding and RYR3 Marker. *Mol. Phylogenet. Evol.* 121, 46–51. doi: 10.1016/j.ympev

Rambaut, A., Drummond, A. J., and Suchard, M. (2013) *Tracer V1.6.* Available at: http://tree.bio.ed.ac.uk/software/tracer/ (Accessed 11 Dec).

Rogers, A. R., and Harpending, H. (1992). Population Growth Makes Waves in the Distribution of Pairwise Genetic Differences. *Mol. Biol. Evol.* 9, 552–569. doi: 10.1093/oxfordjournals.molbev.a040727

Shen, K. N., Jamandre, B. W., Hsu, C. C., Tzeng, W. N., and Durand, J. D. (2011). Plio-Pleistocene Sea Level and Temperature Fluctuations in the Northwestern Pacific Promoted Speciation in the Globally-Distributed Flathead Mullet *Mugil Cephalus. BMC Evol. Biol.* 11, 83. doi: 10.1186/1471-2148-11-83

Shih, N. T., Hsu, K. C., and Ni, I. H. (2010). Age, Growth and Reproduction of Cutlassfishes Spp. In the Southern East China Sea. *J. App. Ichthyol.* 27, 1307–1315. doi: 10.1111/j.1439-0426.2011.01805.x

Sun, P., Chen, Q., Fu, C., Xu, Y., Sun, R., Li, J., et al. (2020b). Latitudinal Differences in Early Growth of Largehead Hairtail (*Trichiurus Japonicus*) in Relation to Environmental Variables. *Fish. Oceanogr.* 29, 470–483. doi: 10.1111/fog.12490

Sun, P., Chen, Q., Fu, C., Zhu, W., Li, J., Zhang, C., et al. (2020a). Daily Growth of Young-of-the Year Largehead Hairtail (*Trichiurus Japonicus*) in Relation to Environmental Variables in the East China Sea. *J. Mar. Syst.* 201, 103243. doi: 10.1016/j.jmarsys.2019.103243

Tajima, F. (1989). Statistical Method for Testing the Neutral Mutation Hypothesis by DNA Polymorphism. *Genetics* 123, 585–595. doi: 10.1093/genetics/123.3.585

Thompson, J. D., Gibson, T. J., Plewniak, F., and Jeanmougin, F. (1997). And Higgins, DThe CLUSTAL_X Windows Interface: Flexible Strategies for Multiple Sequence Alignment Aided by Quality Analysis Tools. *G. Nucleic Acids Res.* 25, 4876–4882. doi: 10.1093/nar/25.24.4876

Tucker, D. W. (1956). Studies on the Trichiuroid Fishes a Preliminary Revision of the Family Trichiuridae. *Bull. Nat. Hist. Mus.* 4, 73–103. doi: 10.5962/p.271719

Tzeng, C. H., Cheng, C. S., and Chiu, T. S. (2007). Analysis of Morphometry and Mitochondrial DNA Sequences From Two *Trichiusus* Species in Waters of the Western North Pacific: Taxonomic Assessment and Population Structure. *J. Fish Biol.* 70, 1–12. doi: 10.1111/j.1095-8649.2007.01368.x

Voris, H. K. (2000). Maps of Pleistocene Sea Levels in Southeast Asia: Shorelines, River Systems and Time Durations. *J. Biogeogr.* 27, 1153–1167. doi: 10.1046/j.1365-2699.2000.00489.x

Wang, P. (1999). Response of Western Pacific Marginal Seas to Glacial Cycles: Paleoceanographic and Sedimentological Features. *Ma. Geol.* 156, 5–39. doi: 10.1016/S0025-3227(98)00172-8

Wang, H. Y., Dong, C. A., and Lin, H. C. (2017). DNA Barcoding of Fisheries Catch to Reveal Composition and Distribution of Cutlassfishes Along the Taiwan Coast. *Fish. Res.* 187, 103–109. doi: 10.1016/j.fishres.2016.11.015

Wang, Y., Jia, X., Lin, Z., and Sun, D. (2011). Responses of Trichiurus Japonicas Catches to Fishing and Climate Variability in the East China Sea. *J. Fish. China* 35, 1881–1889.

Wang, X., Kong, L., Chen, J., Matsukuma, A., and Li, Q. (2017). Phylogeography of Bivalve *Meretrix Petechialis* in the Northwestern Pacific Indicated by Mitochondrial and Nuclear DNA Data. *PloS One* 12, e0183221. doi: 10.1371/journal.pone.0183221

Webb, S. A., Graves, J. A., Macias-Garcia, C., Magurran, A. E., ÒFoighil, D., and Ritchie, M. G. (2004). Molecular Phylogeny of the Livebearing Goodeidae (Cyprinodontiformes). *Mol. Phylogenet. Evol.* 30, 45–56. doi: 10.1016/S1055-7903(03)00257-4

Xu, J., Chan, T. Y., Tsang, L. M., and Chu, K. H. (2009). Phylogeography of the Mitten Crab *Eriocheir Sensu Stricto* in East Asia: Pleistocene Isolation, Population Expansion and Secondary Contact. *Mol. Phylogenet. Evol.* 52, 45–56. doi: 10.1016/j.ympev.2009.02.007

Yang, J. Q., Hsu, K. C., Liu, Z. Z., Su, L. W., Kuo, P. H., Tang, W. Q., et al. (2016). The Population History of *Garra Orientalis* (Teleostei: Cyprinidae) Using Mitochondrial DNA and Microsatellite Data With Approximate Bayesian Computation. *BMC Evol. Biol.* 16, 73. doi: 10.1186/s12862-016-0645-9

Yang, Y., Li, J., Yang, S., Li, X., Fang, L., Zhong, C., et al. (2017). Effects of Pleistocene Sea-Level Fluctuations on Mangrove Population Dynamics: A Less From Sonneratia Alba. *BMC Evol. Biol.* 17, 22. doi: 10.1186/s12862-016-0849-z

Yan, Y. R., Hsu, K. C., Yi, M. R., Li, B., Wang, W. K., Kang, B., et al. (2020). Cryptic Diversity of the Spotted Scat *Scatophagus Argus* (Perciformes: Scatophagidae) in South China Sea: Pre- or Post-Production Isolation. *Mar. Freshwater Res.* 71, 1640–1650. doi: 10.1071/MF19337

Yi, M. R., Hsu, K. C., Gu, S., He, X. B., Luo, Z. S., Lin, H. D., et al. (2022). Complete Mitogenomes of Four Trichiurus Species: A Taxonomic Review of the *T. Lepturus* Species Complex. *Zookeys* 1084, 1–26. doi: 10.3897/zookeys.1084.71576

Yi, M. R., Hsu, K. C., Luo, Z. S., Gu, S., Feng, B., Lin, H. D., et al. (2021a). Diversity of the Family Apogonidae Along the Northwestern Coastline of the South China.A. Sea. *Cah. Biol. Mar.* 62, 381–391. doi: 10.21411/CBM.A.A90D1ED2

Yi, M. R., Hsu, K. C., Wang, J. X., Feng, B., Lin, H. D. , and Yan, Y. R. (2021b). Genetic Structure and Diversity of the Yellowbelly Threadfin Bream Nemipterus Bathybius in the Northern South China Sea *Diversity* 13,324. doi: 10.3390/d13070324

Zheng, S. Y., Liu, J. H., and Jia, P. F. (2019). Complete Mitogenome of the Cutlassfish *Trichiurus Haumela* (Scombriformes: Trichiuridae) From Ningde, Fujian Province, Southeast China. *Mitochondrial DNA B.* 4, 87–88. doi: 10.1080/23802359.2018.1536475

Zhong, P. H., Shao, M. Q., Dai, N. H., and Zheng, F. W. (2009). Genetic Differentiation of Tegillarca Granosa Based on Mitochondrial COI Gene Sequences. *Zool. Res.* 30, 17–23. doi: 10.3724/SP.J.1141.2009.01017